

# Role of $\Delta$ exchange for $p\bar{p}$ annihilation into two-pion and three-pion channels

M. Betz<sup>a\*</sup>, E. A. Veit<sup>a†</sup>, and J. Haidenbauer<sup>b‡</sup>

<sup>a</sup>*Instituto de Física - Universidade Federal do Rio Grande do Sul*

*Cx. P. 15051; CEP 91501-970, Porto Alegre, Brazil*

<sup>b</sup>*Institut für Kernphysik, Forschungszentrum Jülich GmbH,  
D-52425 Jülich, Germany*

## Abstract

$p\bar{p}$  annihilation into two pions and three pions is studied in a baryon-exchange model. Annihilation diagrams involving nucleon as well as  $\Delta$ -resonance exchanges are included consistently in the two- and three-pion channels. Effects from the initial-state interaction are fully taken into account. A comparison of the influence of the  $\Delta$  exchange on the considered annihilation channels is made and reveals that its importance for three-pion annihilation is strongly reduced as compared to two-pion annihilation. It is found that annihilation into three uncorrelated pions can yield up to 10% of the total experimentally observed three-pion annihilation cross section.

PACS number(s): 13.75.Cs, 14.20.-c, 21.30.Cb, 25.43.+t

Typeset using REVTEX

---

\*Email: betz@if.ufrgs.br

†Email: eav@if.ufrgs.br

‡Email: j.haidenbauer@fz-juelich.de

## I. INTRODUCTION

Nucleon-antinucleon ( $N\bar{N}$ ) annihilation has attracted a great deal of interest over the past two decades [1,2]. Although recently the main emphasis has often been put on meson spectroscopy and specifically the identification of exotic mesonic states [3], one should not forget that this process also offers a rich field in which various aspects of quark-gluon dynamics and/or hadron dynamics can be tested. Indeed the development of a microscopic model which describes the  $N\bar{N}$  interaction and, at the same time, can account also for all phenomena associated with the  $N\bar{N}$  annihilation into two, three, ..., mesons is a rather challenging task for any theorist and has so far not been achieved. With regard to  $N\bar{N}$  annihilation, models based on quark degrees of freedom were the first ones to be utilized in attempts to obtain a quantitative description of annihilation into two and three mesons. Their use was prompted by the expectation that annihilation processes might be a good place for detecting explicit quark-gluon effects since relatively short interaction ranges are involved. The pioneering works stem from Maruyama and Ueda [4] and Green and Niskanen [5], followed by an impressive series of studies carried out by the Tübingen group [6]. (Cf. also Ref. [1] for a comprehensive review of quark-model studies of  $N\bar{N}$  annihilation.)

Investigations of  $N\bar{N}$  annihilation relying on the more traditional meson-baryon picture, where the annihilation process is described by baryon-exchange diagrams, were initiated by Moussallam not long after the first works within the quark model had appeared [7]. Subsequently, the Jülich group carried out several studies based on this approach [8,9] and more recently also Yan and Tegen [10,11]. Those works indicate that the conventional hadronic concept for describing  $N\bar{N}$  annihilation is capable of producing results that are at least of the same quality as obtained from quark-gluon models. However, all those studies concentrated on two-meson annihilation channels only. This is certainly an unsatisfying situation because it would be interesting to see whether the baryon-exchange picture of  $N\bar{N}$  annihilation works similarly well for three-meson decay as it does for the two-meson channels. Furthermore, we wish to recall that the latest model by the Jülich group [9] constitutes already an essential step in achieving a unified description of  $N\bar{N}$  scattering and annihilation. In this model the elastic and annihilation parts of the  $N\bar{N}$  interaction are derived in a consistent framework and, in addition, the transitions to two-meson channels,  $N\bar{N} \rightarrow M_1 M_2$ , and the contributions of these two-meson channels to the total  $N\bar{N}$  annihilation are described consistently as well. Thus, it is important, but also challenging, to go a step further and include the three-meson decay channels explicitly as well in this model.

In a series of recent works [12–15], we have used the baryon-exchange model to investigate proton-antiproton annihilation into three uncorrelated pions. By “uncorrelated”, we mean that these pions are not the decay products of an intermediate heavy-meson resonance. Of course, annihilation into three pions is known to be dominated by the formation and decay of intermediate states made up of a pion and a heavy meson, and such processes have already been studied in the baryon-exchange model. The process at hand only constitutes a relatively small background. Yet such background contributions have been found significant in phenomenological analyses of  $p\bar{p}$  annihilation into  $\pi^+\pi^-\pi^0$  at rest [16,17] and it can be expected that they need to be also taken into account in precise analyses of annihilation into three neutral pions, which has recently been the object of considerable interest [18–20].

Our investigation of annihilation into three uncorrelated pions was done in a distorted-

wave Born approximation (DWBA), employing the most recent  $N\bar{N}$  model of the Jülich group [9] for the initial-state interaction, and guided by the same principles applied in that reference for the calculation of annihilation into two-meson channels. The work was initiated with a study of the  $p\bar{p} \rightarrow \pi^+\pi^-\pi^0$  process [12], in a simplified model, in which only nucleon exchange was included explicitly in the annihilation amplitude. The effect of  $\Delta$  exchange – which is known to produce a significant enhancement of the cross-section for annihilation into two pions [7,10] – was taken into account in an approximate phenomenological fashion, namely through a readjustment of the cutoff at the  $NN\pi$  vertex. In a subsequent paper [13], a first step in assessing the shortcomings of this simplification was made by comparing the pertinent results with those obtained through explicit inclusion of the amplitudes involving the exchange of one  $N$  and one  $\Delta$ . Very recently, a further step was taken with the inclusion of the annihilation amplitude generated by double  $\Delta$  exchange [14,15].

Despite those achievements we have to concede, however, that there is still an inconsistency in our calculations so far. The nucleon-antinucleon interaction developed by the Jülich group is derived in a time-ordered formalism and specifically also the amplitude for annihilation into two pions is calculated in time-ordered perturbation theory. In contrast, in order to avoid the proliferation of diagrams, the three-pion annihilation amplitude is calculated in Feynman-type perturbation theory. This procedure implies that the treatment of the off-shell behaviour of the three-pion annihilation amplitude is different from that used in the Jülich model of annihilation into two pions [9]. This shortcoming has been previously ignored. However, it is of relevance now that we are able to calculate the two-pion and three-pion annihilation channels involving  $N$  as well as  $\Delta$  exchange in a consistent way. Therefore, we decided to treat the two-pion annihilation amplitude in the same fashion as the three-pion one, i.e. in Feynman-type perturbation theory. Clearly, in such an approach  $NN\pi$  and  $N\Delta\pi$  vertex parameters taken from the work of the Jülich group will no longer reproduce the phenomenology of two-pion annihilation and a refitting is therefore necessary. This means, in turn, that full consistency with the Jülich  $N\bar{N}$  model, which we continue to use as the initial-state interaction, will be lost. But this is excusable to a certain extent because the annihilation channel in question,  $N\bar{N} \rightarrow 2\pi$ , yields only a tiny contribution to the total  $N\bar{N}$  annihilation cross section [9]. On the other hand, the  $NN\pi$  and  $N\Delta\pi$  vertex parameters play a crucial role for the  $N\bar{N} \rightarrow 3\pi$  cross section, as we will see and explore in the present paper, and therefore it is rather important to constrain them by the requirement of consistency between the two- and three-pion annihilation channels.

In this paper we present results of a combined study of proton-antiproton annihilation into two and three pions in a baryon-exchange model. We start out from the two-pion annihilation channel. We use available experimental data on  $p\bar{p} \rightarrow \pi^+\pi^-$  to determine the free parameters of our model, i.e. the cutoff masses in the form factors at the  $NN\pi$  and  $N\Delta\pi$  vertices. The effects of different choices for the analytical form of those vertex form factors are explored as well. We then turn to three-pion annihilation and discuss the relative importance of  $NN$ ,  $N\Delta$  and  $\Delta\Delta$  exchanges.

In Sec. II we provide some details of our model. In particular, we specify the ingredients used for evaluating the  $N$ - and  $\Delta$ -exchange diagrams for  $N\bar{N}$  annihilation into two and three pions, i.e. the baryon-baryon-meson Lagrangians and the corresponding vertex form factors and coupling constants. Furthermore we give a short description of the  $N\bar{N}$  model that is employed for the initial-state interaction and we outline how the amplitudes for  $N\bar{N}$

annihilation into two and three pions are determined in distorted-wave Born approximation. Our results are presented and discussed in Sec. III. First we consider the reaction  $p\bar{p} \rightarrow \pi^+\pi^-$  which is used for fixing the free parameters of our model. Subsequently, we examine the reaction  $p\bar{p} \rightarrow \pi^+\pi^-\pi^0$  as well as annihilation channels involving only neutral pions ( $p\bar{p} \rightarrow \pi^0\pi^0$ ,  $p\bar{p} \rightarrow \pi^0\pi^0\pi^0$ ). We show results for total and differential cross sections and also for branching ratios from specific initial  $N\bar{N}$  states. The paper ends with some concluding remarks.

## II. THE MODEL

### A. Distorted-wave Born approximation

The basis of the present work is the Jülich model for  $N\bar{N}$  scattering and annihilation [9]. In this model heavier mesons are treated as stable particles in the (successful) description of  $N\bar{N}$  annihilation into two mesons. In accordance with this approach, the uncorrelated three-pion channel is here considered separately from the channels in which a pion and a heavy meson, which can decay into two pions, are formed. When calculating the total cross section for annihilation into three pions, the contributions from these channels are added incoherently. Neglecting interferences between the various channels seems acceptable for the aim of this work, which is to perform an exploratory study about the relevance of the uncorrelated three-pion channel for the annihilation cross section.

The general procedure is to start from the Born transition amplitude  $V^{N\bar{N} \rightarrow n\pi}$  for annihilation into  $n$  ( $= 2$  and  $3$ ) pions and include the initial-state interaction in distorted-wave Born approximation, so that the annihilation amplitude  $T^{N\bar{N} \rightarrow n\pi}$  is given by

$$T^{N\bar{N} \rightarrow n\pi} = V^{N\bar{N} \rightarrow n\pi} + V^{N\bar{N} \rightarrow n\pi} G^{N\bar{N} \rightarrow N\bar{N}} T^{N\bar{N} \rightarrow N\bar{N}}, \quad (1)$$

where  $G^{N\bar{N} \rightarrow N\bar{N}}$  is the propagator for the  $N\bar{N}$  pair. The  $N\bar{N}$  scattering amplitude  $T^{N\bar{N} \rightarrow N\bar{N}}$  is obtained from the solution of a Lippmann-Schwinger equation [9]

$$T^{N\bar{N} \rightarrow N\bar{N}} = V^{N\bar{N} \rightarrow N\bar{N}} + V^{N\bar{N} \rightarrow N\bar{N}} G^{N\bar{N} \rightarrow N\bar{N}} T^{N\bar{N} \rightarrow N\bar{N}}. \quad (2)$$

In the work of the Jülich group the time-ordered formalism is invoked to cast Eqs. (1) and (2) in tractable (three-dimensional) form. The  $N\bar{N}$  interaction  $V^{N\bar{N} \rightarrow N\bar{N}}$  and, in particular, the Born transition amplitudes for annihilation into two mesons are likewise calculated within time-ordered perturbation theory (TOPT). Here however, in order to avoid the evaluation of the numerous graphs that occur within TOPT for the Born transition amplitude  $V^{N\bar{N} \rightarrow 3\pi}$  for annihilation into three pions, we prefer to employ Feynman diagrams. We stress that these two procedures imply different off-shell extrapolations of the annihilation amplitudes and are therefore not equivalent. Since we intend to use annihilation into two pions for the determination of the free parameters in our model, we need to maintain consistency between our treatments of annihilation into two and three pions. Therefore, we will use the Feynman prescription also to calculate the Born transition amplitude  $V^{N\bar{N} \rightarrow 2\pi}$  for annihilation into two pions. Only the initial-state scattering amplitude  $T^{N\bar{N} \rightarrow N\bar{N}}$  will be still computed in time-ordered formalism.

In the case of annihilation into two pions, the amplitudes may be expanded in partial waves and the angular distribution and integrated cross section calculated in standard fashion. In the case of annihilation into three pions, the Monte Carlo method is used to perform the final phase-space integration.

## B. Annihilation amplitudes

In accordance with the Jülich  $N\bar{N}$  model we assume that the dynamics of annihilation into pions is mediated by nucleon and  $\Delta$  exchanges. Hence, the Born transition amplitudes  $V^{N\bar{N} \rightarrow n\pi}$  ( $n = 2, 3$ ) are given by the sums of the Feynman tree diagrams involving the  $NN\pi$ ,  $\Delta N\pi$  and  $\Delta\Delta\pi$  vertices, shown in Fig. 1 and Fig. 2. The complete amplitudes are obtained by summing such diagrams over all permutations of the final-state pions.

The contributions of the various diagrams are evaluated using standard interaction Lagrangians, namely

$$\mathcal{L}_{NN\pi} = \frac{f_{NN\pi}}{m_\pi} \bar{\psi}_N \gamma^5 \vec{\tau} \cdot \vec{\partial} \phi \psi_N , \quad (3)$$

$$\mathcal{L}_{\Delta N\pi} = \frac{f_{\Delta N\pi}}{m_\pi} \bar{\psi}_\Delta^\mu \vec{T} \cdot \partial_\mu \vec{\phi} \psi_N + h.c. , \quad (4)$$

$$\mathcal{L}_{\Delta\Delta\pi} = -\frac{f_{\Delta\Delta\pi}}{m_\pi} \bar{\psi}_{\Delta\mu} \gamma^5 \vec{I} \cdot \vec{\partial} \phi \psi_\Delta^\mu , \quad (5)$$

where  $\vec{I}$  is the  $\Delta$  isospin operator and  $\vec{T}$  the  $N \rightarrow \Delta$  transition isospin operator (we use the normalization conventions of Ref. [21] for these operators).

The corresponding vertex factors in Feynman diagrams are:

$$\mathcal{V}_{NN\pi} = -\frac{f_{NN\pi}}{m_\pi} \gamma^5 \tau^i \not{q} , \quad (6)$$

$$\mathcal{V}_{\Delta N\pi} = -\frac{f_{\Delta N\pi}}{m_\pi} q_\mu T^i + h.c. , \quad (7)$$

$$\mathcal{V}_{\Delta\Delta\pi} = \frac{f_{\Delta\Delta\pi}}{m_\pi} g_{\mu\nu} \gamma^5 I^i \not{q} , \quad (8)$$

where  $q_\mu$  is the pion four-momentum and the index  $i$  specifies the pion isospin. The nucleon propagator takes the standard form

$$iG_N(p) = i \frac{\not{p} + m_N}{p^2 - m_N^2} . \quad (9)$$

For the  $\Delta$  propagator, we adopt [22]

$$iG_\Delta^\mu(p) = -i \frac{\not{p} + m_\Delta}{p^2 - m_\Delta^2} \Theta^{\mu\nu}(p) , \quad (10)$$

with

$$\Theta^{\mu\nu}(p) \equiv g^{\mu\nu} - \frac{\gamma^\mu \gamma^\nu}{3} - \frac{2p^\mu p^\nu}{3m_\Delta^2} + \frac{p^\mu \gamma^\nu - p^\nu \gamma^\mu}{3m_\Delta} . \quad (11)$$

Two of the coupling constants appearing in the above vertices are already used in the Bonn potential [23] and Jülich  $N\bar{N}$  model [9], namely  $f_{NN\pi}^2/4\pi = 0.0778$  and  $f_{\Delta N\pi}^2/4\pi = 0.224$ . For the  $\Delta\Delta\pi$  coupling, we shall rely on the  $SU(2) \times SU(2)$  quark–model relation [24],  $f_{\Delta\Delta\pi} = \frac{9}{5}f_{NN\pi}$ . This gives  $f_{\Delta\Delta\pi}^2/4\pi = 0.252$ .

Form factors must be included in order to regularize the calculation and to take into account the extended hadron structure. We know from our experience with other hadronic reactions that the results might depend sensitively on those form factors, in particular when loop integrations like in Eq. (1) are involved. Therefore, in order to investigate the sensitivity of our model to the details of these form factors, we employ three different parametrizations in the present study. In two of these we follow the conventional assumption that the vertex form factor depends only on the momentum of the exchanged particle, i.e. the particle which is off-shell in the Born diagram. For annihilation into three pions, the inner vertex contains the product of two such form factors since there are two off-shell particles attached to this vertex. Explicitly, we employ the functions

$$\mathcal{F}_M(p) = \frac{\Lambda_{\alpha X\pi}^2 - M_X^2}{\Lambda_{\alpha X\pi}^2 - p^2} \quad (12)$$

and

$$\mathcal{F}_G(p) = \exp\left[-\frac{(p^2 - M_X^2)^2}{\Lambda_{\alpha X\pi}^4}\right]. \quad (13)$$

In these expressions,  $X$  stands for the type ( $N$  or  $\Delta$ ) of the exchanged off-shell particle,  $M_X$  for its mass and  $p$  for its four-momentum;  $\alpha$  denotes the type of the other baryon present at the vertex and  $\Lambda_{\alpha X\pi}$  represents the cutoff mass corresponding to the  $\alpha X\pi$  vertex. In principle, four independent cutoff masses have to be specified: one for the  $NN\pi$  vertex, characterizing an off-shell nucleon, two for the  $\Delta N\pi$  vertex, characterizing an off-shell nucleon or an off-shell  $\Delta$ , respectively, and one for the  $\Delta\Delta\pi$  vertex, characterizing an off-shell  $\Delta$ . In order to reduce the number of free parameters, we assume  $\Lambda_{N\Delta\pi} = \Lambda_{\Delta N\pi} = \Lambda_{\Delta\Delta\pi} \equiv \Lambda_\Delta$ . The procedure for fixing the values of the remaining independent cutoff parameters ( $\Lambda_{NN\pi} \equiv \Lambda_N$  and  $\Lambda_\Delta$ ) will be discussed in Sec. III. In the following we will refer to those form factors as monopole [Eq. (12)] and Gaussian [Eq. (13)], respectively.

The third type of regularization we consider attributes a damping factor to each line in the Born diagrams, including the external legs. Specifically we use a parametrization introduced by B. Pearce [25] and later by C. Schütz [26] in their studies of the  $\pi N$  system which is given by

$$\mathcal{F}_P(p) = \frac{\Lambda_X^4}{\Lambda_X^4 + (p^2 - M_X^2)^2}, \quad (14)$$

with  $\Lambda_X$  the cutoff mass associated with a baryon line of type  $X$ . Note that, in principle, a similar factor should be applied to the pion lines as well. But since in our DWBA calculation the pions are always on their mass shell this factor will be identical to 1 and, therefore, can be omitted. In the following we will refer to this choice as the Pearce form factor.

In order to combine the Feynman annihilation amplitudes with the initial-state distorted wave, it is necessary to specify a prescription for the energy components of the four-momenta of their external  $N$  and  $\bar{N}$  legs. We set both equal to their on-energy-shell value (i.e., half the total available energy in the center-of-mass frame).

### C. Initial-state interaction

The  $N\bar{N}$  interaction  $V^{N\bar{N} \rightarrow N\bar{N}}$  used to obtain the initial-state distorted wave is that developed in Ref. [9], without modification. For completeness, we summarize here its main features.

The interaction is made up of an elastic and an annihilation part:

$$V^{N\bar{N} \rightarrow N\bar{N}} = V_{el} + V_{ann}. \quad (15)$$

The elastic interaction is obtained through a G-parity transformation of the full Bonn  $NN$  potential [23], corresponding to the diagrams shown in Fig. 3.

The annihilation interaction consists of a microscopic and a phenomenological piece:

$$V_{ann} = \sum_{ij} V^{M_i M_j \rightarrow N\bar{N}} G^{M_i M_j} V^{N\bar{N} \rightarrow M_i M_j} + V_{opt}. \quad (16)$$

The microscopic component is the sum of box diagrams with two-meson intermediate states resulting from all possible combinations of  $\pi$ ,  $\eta$ ,  $\rho$ ,  $\omega$ ,  $a_0$ ,  $f_0$ ,  $a_1$ ,  $f_1$ ,  $a_2$ ,  $f_2$ ,  $K$  and  $K^*$  mesons (Fig. 4a). The transition potentials  $V^{N\bar{N} \rightarrow M_i M_j}$  are given by the baryon-exchange diagrams presented in Fig. 5. The coupling constants and cutoff parameters at the vertices of these transition potentials are quoted in Table I of Ref. [9]. Note that in Ref. [9] these transition potentials are employed also for the calculation of the amplitudes for annihilation into a pion and a heavy meson  $M$ . Those amplitudes are obtained from equations analogous to Eq. (1), with  $V^{N\bar{N} \rightarrow \pi M}$  as the Born term. The corresponding contributions to the cross sections for annihilation into three pions will be used here without modification.

The phenomenological optical potential (Fig. 4b) simulates the effect of contributions from annihilation into more than two mesons, and is parametrized in coordinate space as

$$V_{opt} = -iW \exp\left(-\frac{r^2}{2r_0^2}\right), \quad (17)$$

with  $W = 1$  GeV and  $r_0 = 0.4$  fm. These values have been obtained [9] through an overall fit to  $N\bar{N}$  integrated cross-section data.

## III. RESULTS AND DISCUSSION

As mentioned in the Introduction, in a previous publication [12] aimed at acquiring a first idea of the relevance of the uncorrelated channel to the  $p\bar{p} \rightarrow \pi^+ \pi^- \pi^0$  cross section,  $\Delta$  exchange was not included in the transition amplitude. This, of course, is at variance with the dynamics included in the treatment of the  $N\bar{N} \rightarrow 2\pi$  amplitude, where  $\Delta$  exchange is taken into account. The argument invoked was that if one considers only the (dominant) charged two-pion channel, one finds that the effect of  $\Delta$  exchange can be described phenomenologically by using an effective value for the cutoff at the  $NN\pi$  vertex. It turned out that, in this rather crude treatment, the uncorrelated channel adds a 10% contribution to the total  $p\bar{p}$  annihilation cross section into three pions, motivating a more systematic study. In subsequent studies, the exchange of one  $\Delta$  [13], and of two  $\Delta$ 's [14] has been explored.

While this unified the dynamics of annihilation into two and three pions, complete consistency was not achieved yet, since the two-pion channel was treated with TOPT [9] while for the three-pion channel, the Feynman prescription was used [13,14]. More recently [15], first results of a calculation in which both two-pion and three-pion channels are treated within the Feynman prescription were presented. Here we explore more fully the predictions of this model. Specifically we analyze the contributions of the uncorrelated three-pion channel not only to the charged but also to the neutral annihilation cross sections, and we show predictions for various branching ratios as well. We also investigate the effect of various choices of the vertex form factors on our results and we explore the importance of the contributions coming from the  $\Delta$ -exchange diagrams.

### A. $p\bar{p} \rightarrow \pi^+\pi^-$ cross section

To get insight into the influence of the vertex form factors on the results for  $p\bar{p} \rightarrow 3\pi$  we accomplished fits to the reaction  $p\bar{p} \rightarrow \pi^+\pi^-$  using each of the three parametrizations introduced in Sec. II B. Since it turned out that the presently available data do not allow to determine the relative magnitudes of the  $N$  and  $\Delta$  exchange contributions unambiguously, we prepared two sets of models, one with  $\Lambda_N$  larger than  $\Lambda_\Delta$  and the other with  $\Lambda_N$  smaller than  $\Lambda_\Delta$ . Thus, we have in total six parameter sets, all determined in such a way as to provide an adequate description of the total and differential  $p\bar{p} \rightarrow \pi^+\pi^-$  cross sections. The resulting values for the cutoff masses are compiled in Table I. The parameter set A corresponds to form factors which suppress  $\Delta$  exchange compared to nucleon exchange. The parameter set B corresponds to a quite strong  $\Delta$  exchange, hopefully providing some sort of upper bound for the  $\Delta$  contribution when used to describe annihilation into three uncorrelated pions later on.

The results for the  $p\bar{p} \rightarrow \pi^+\pi^-$  total cross sections are compared to the data [27–29] in Fig. 6. Considering the rather large experimental errors at low energy, all parameter sets can be said to provide an adequate description. The relative importance of  $N$  and  $\Delta$  exchanges is illustrated in Table II, which shows their separate contributions to the cross section at two sample energies. For the parameter set A the contribution from  $\Delta$  exchange is indeed not very important. Turning it off reduces the cross sections by – at most, depending on the energy – 30% (Pearce form factor) to 10% (monopole form factor). For the Gaussian form factor, the reduction is by about 20%. For the parameter set B, the  $\Delta$ -exchange contribution dominates over the  $N$  contribution, although, because of the constructive interference between them, both contributions are important in building up the cross section. One should note that the relative importance of  $N$  and  $\Delta$  exchanges results in general from a balance between two competing effects. On the one hand, the larger coupling constant at the  $\Delta N\pi$  vertex favors  $\Delta$  exchange over  $N$  exchange, but on the other hand, since the relevant kinematical region for the exchanged particle is space-like, it is somewhat further away from the on-shell point for the  $\Delta$  than for the nucleon. This leads to a comparatively larger propagator denominator and a stronger damping due to form factors for the  $\Delta$ .

The angular distributions are shown in Fig. 7 for two incident momenta. The quality of the results for other measured incident momenta is similar to that of these two sample cases.

For forward scattering, the differential cross section looks reasonable for all parameter sets. For larger incident momenta, a stronger  $\Delta$  contribution tends to produce a bending down of the cross section at small angles (see the case  $p_{lab} = 679$  MeV/c with parameter set B). This imposes an upper limit on the amount of  $\Delta$  contribution which is acceptable. Let us note, however, that the data at somewhat higher energies do indeed show such a bending down in the forward direction [30]. With respect to backward scattering our models fare rather poorly. But this is expected and therefore not a reason of concern. It is known that final-state interactions, not considered here, play an important role for backward angles and do improve the results significantly [31]. Also, it has been argued [10] that a tensor coupling for the  $N\Delta\pi$  vertex would enhance the differential cross section around  $100^\circ$  for  $p_{lab} > 680$  MeV/c.

## B. $p\bar{p} \rightarrow \pi^+\pi^-\pi^0$ annihilation

### 1. Cross section

The  $p\bar{p}$  annihilation into three pions has contributions from three uncorrelated pions in addition to some two-meson channels, involving a heavier meson ( $\rho$ ,  $f_o$  and  $f_2$ ), which decays subsequently into two pions with some branching ratio (100%, 78% and 85%, respectively). The two-meson channels have already been studied with the Jülich model by Mull et al. [9]. Here we concentrate on the uncorrelated three-pion contribution to the  $p\bar{p} \rightarrow \pi^+\pi^-\pi^0$  cross section.

Our results are shown in Table III for the six parameter sets of Table I, at two sample energies. For parameter set A most of the cross section comes from  $N$  exchange and the contributions from one- and two- $\Delta$  exchanges are negligible. For parameter set B, however, the one- and two- $\Delta$  exchanges are sizeable. Especially for the Pearce form factor, the cross section is enhanced by almost a factor of two when the  $\Delta$ -exchange contributions are added. On the other hand, the overall magnitude of the cross sections is, in general, much smaller for set B than for set A, indicating that the increase due to the  $\Delta$ -exchange contribution for set B is by far not sufficient to compensate the reduction of the  $N$ -exchange contribution. This means that the relative importance of annihilation via  $\Delta$  exchange as compared to  $N$  exchange is much smaller in the reaction  $p\bar{p} \rightarrow \pi^+\pi^-\pi^0$  than it is for  $p\bar{p} \rightarrow \pi^+\pi^-$ . One reason for this is that the number of possible charge combinations of the exchanged baryons is larger for amplitudes involving  $\Delta$ 's and the interferences between their contributions tend to be destructive. The differences between the results obtained with different form factors are also easily understood qualitatively. For the Pearce type, since the factors are in effect associated with propagators, there is one more factor for the three-pion annihilation amplitude, compared to the two-pion one. For the other types, however, the factors are associated with internal vertex legs and therefore two more factors appear in the three-pion amplitude. This makes the Pearce form factor to yield less suppression for annihilation into three pions. When two baryons are exchanged, each one of them is not as far off shell as when only one is exchanged. Therefore, because of its stronger variation with  $p^2$ , the Gaussian form cuts off less strongly for three-pion annihilation than the monopole form factor.

The total experimental  $p\bar{p} \rightarrow \pi^+\pi^-\pi^0$  cross section ranges from around 7 mb to 3 mb for energies from 65 MeV to 220 MeV [27]. In comparison to these values, the calculated uncorrelated cross section varies from mere insignificance (for monopole and Gaussian form factors with parameter set B), to about 10% of the measured total cross section for the Gaussian form factor with parameter set A. The relevance of the contribution from annihilation into three uncorrelated pions might be best seen from Fig. 8, where our results for the three uncorrelated pions are added to Mull's results [9] for annihilation into two-meson channels ( $\rho\pi$ ,  $f_o\pi$  and  $f_2\pi$ ), weighted with the percentages of decay of the heavy mesons into two pions and the isospin factors, and compared with the total experimental annihilation cross section.

## 2. Branching ratios

A more detailed comparison can be made by considering the experimental information from a specific antiprotonium initial state. Annihilation of antiprotonic hydrogen atoms into  $\pi^+\pi^-\pi^0$  has been studied by stopping antiprotons from LEAR in hydrogen gas by the ASTERIX Collaboration [17]. All  $N\bar{N}$  initial states for  $S$  and  $P$  waves which may decay into  $\pi^+\pi^-\pi^0$  have been considered<sup>1</sup>, namely  $^3S_1 (I=0)$ ,  $^1S_0 (I=1)$ ,  $^1P_1 (I=0)$ ,  $^3P_1 (I=1)$  and  $^3P_2 (I=1)$ . The phenomenological analysis has been made in terms of resonant amplitudes and a non-resonant (phase-space) background. The contributions from the  $\rho\pi$  channel have already been compared with the results of the Jülich model [32]. The phase-space component has also been compared with the uncorrelated three-pion contribution in the first, simplified version of our model, in which  $\Delta$  exchange was not considered explicitly. Here we use the present model to compare our results with the experimental values.

As before [12,32], we assume that all the spin states of a given orbital angular momentum in protonium are populated with about the same probability and identify the relative branching ratios for decay from a given atomic state to the ratios between the contributions from the corresponding partial waves to the annihilation cross section at low energy. Although the cross sections themselves vary rapidly with energy, these ratios are almost constant for small laboratory energies (a few MeV). Thus, like in our previous work, we use cross-section ratios at 5 MeV.

Table IV shows our results for the ratios of branching ratios for  $N\bar{N} \rightarrow \pi^+\pi^-\pi^0$  for various types of form factors and parameter sets, compared to the experimental values extracted from the phenomenological analysis of Ref. [17]. An estimate based on ratios between numbers  $(2J+1)$  of available states is given as well.

Not surprisingly, for parameter set A, where  $N$  exchange is dominant, the results are very similar to our previous ones [12], where  $\Delta$  exchange had not been considered at all. The theoretical  $^3S_1/^1S_0$  ratios depend only weakly on the dynamics. The predictions are close to the value 3, which is expected on the basis of simple state counting, though they

---

<sup>1</sup>The  $G$ -parity of the initial antiprotonium state is  $G = (-1)^{L+S+I}$ , and for a three-pion final state  $G = -1$ ; this determines the isospin quantum number  $I$  for each allowed initial state. The  $^3P_0$  initial state is forbidden by angular momentum and parity conservation.

tend to be, in general, somewhat larger than this phenomenological value, especially for the Pearce form factor. The theoretical  $^3P_1/{}^1P_1$  ratios show some dependence on the spin and isospin dynamics and are smaller than the results of the phenomenological analysis by a factor of about 2. For the  $^3P_2/{}^1P_1$  ratio, the theoretical results again depend weakly on the dynamics; however, they also fall short of the experimental evidence by a factor of 2 to 3.

For parameter set B, where  $\Delta$  exchange is also relevant, the  $^3S_1/{}^1S_0$  ratios show the same general trends as for set A, although the result for the Pearce form factor is now considerably larger than the experimental value. The  $^3P_1/{}^1P_1$  and  $^3P_2/{}^1P_1$  ratios, on the other hand, are spectacularly larger than for set A and now overshoot the experimental data by far. This effect originates from the fact that, with our choices of vertices and propagators, exchanges involving  $\Delta$ 's make a very small contribution to the  ${}^1P_1$  partial wave. Consequently, if form factors are chosen such as to suppress the  $NN$ -exchange contribution (as is the case for set B), the total contribution of that partial wave to the cross section is small and the  $^3P_1/{}^1P_1$  and  $^3P_2/{}^1P_1$  ratios are large. The fact that the experimental values for these ratios lie between our results for sets A and B is in accordance with our objective of these sets as extremes between which realistic values for the cutoffs are confined.

### C. Annihilation into neutral pions

Some experimental results for  $p\bar{p}$  annihilation into neutral pions have been published already a long time ago [33]. But only very recently, for the first time, data at beam momenta below 1 GeV/c have been made available by the Crystal Barrel Collaboration for annihilation into  $2\pi^0$ 's [34,35]. Specifically, their measurement at a laboratory momentum of 600 MeV/c is still within the limit of validity of our model and, therefore, it is possible to compare our results with those data, as we shall do in this section. We emphasize that all our parameter sets were fixed by the annihilation into two charged pions, as discussed above. Thus, the results presented here for the reactions  $p\bar{p} \rightarrow 2\pi^0$  as well as  $p\bar{p} \rightarrow 3\pi^0$  are genuine predictions of our model.

#### 1. $p\bar{p} \rightarrow 2\pi^0$ annihilation

For the reaction  $p\bar{p} \rightarrow 2\pi^0$  there are high-statistics data taken at LEAR in the momentum range 600-1940 MeV/c [34]<sup>2</sup>. In Fig. 9, we compare the differential cross sections predicted by our model with the data of Ref [34] at the laboratory momentum  $p_{lab} = 600$  MeV/c. (The next higher energy measured,  $p_{lab} = 900$  MeV/c, is already beyond the validity range of our model and therefore we refrain from comparing our model with those data.) Note that the normalization is such that the area under the curve times  $2\pi$  gives the corresponding total annihilation cross section.

---

<sup>2</sup> These data show a systematic disagreement in normalization with the earlier data [33], i.e. the cross sections are a factor of more than 2 larger.

It can be seen that the predictions for the differential cross section at small angles are reasonable for parameter set A, i.e. for the models where nucleon exchange is the dominant annihilation process. However, for parameter set B, which corresponds to models with a large contribution from  $\Delta$  exchange, we observe a serious disagreement with the data. Obviously the  $\Delta$  exchange tends to bend down the differential cross section at small angles, something which we also noticed for the charged case. For angles near  $90^\circ$  the Pearce form factor yields a contribution too high for both parameter sets whereas all other models are in rough agreement with the data.

Predictions at a lower laboratory momentum,  $p_{lab} = 360$  MeV/c, are also shown in Fig. 9 though at this energy there are presently no data available.

The experimental total cross section for  $p\bar{p} \rightarrow \pi^0\pi^0$  given in Ref. [34] was obtained by integrating only over the limited range  $\cos(\theta) = 0$  to 0.85. Thus, we do the same for obtaining the theoretical cross sections at  $p_{lab} = 600$  MeV/c, which are compiled in Table V. The model predictions range from values close to the experimental ones, to values that are too large by a factor of 2 to 3. The contributions from the individual annihilation mechanisms ( $N$  and  $\Delta$  exchange, respectively) are listed in Table VI for all considered parameter sets. Not unexpectedly, the general features are very similar to those found for the annihilation into two charged pions.  $N$  exchange dominates in case of parameter set A, while  $\Delta$  exchange provides the larger contribution for the parameter set B. The interference between  $N$  and  $\Delta$  exchanges is generally constructive.

## 2. $p\bar{p} \rightarrow 3\pi^0$ annihilation

Our results for the cross section for  $p\bar{p}$  annihilation into three uncorrelated neutral pions at  $p_{lab} = 600$  MeV/c are compiled in Table VII. The values range from  $2.2 \mu b$  (for parameter set B with monopole form factor) to  $37.8 \mu b$  (for parameter set A with Gaussian form factor). The corresponding experimental value for the total annihilation cross section (which includes contributions from three uncorrelated pions as well as from two-meson annihilation channels that finally decay into three pions) is  $356 \pm 18 \mu b$  [20]. Thus, like already for the case of charged pions, it turns out that the annihilation into three uncorrelated  $\pi^0$ 's could amount to up to 10% of the total  $3\pi^0$  annihilation cross section. This suggests that such a “non-resonant background” contribution should perhaps be included in detailed phenomenological analyses aimed at identifying new hadronic states [18–20].

The contributions from the individual annihilation mechanisms can be seen in Table VIII. As for the charged case, it turns out that annihilation via  $N\Delta$  as well as via double- $\Delta$  exchange is negligible for parameter set A. For parameter set B,  $NN$  and  $N\Delta$  exchanges yield similar contributions, while  $\Delta\Delta$  exchange remains practically negligible. However, the overall size of the cross-section is again much less than for set A. The comparison made in Sec. III B 1 between the various types of form factors applies to the present case also.

## IV. SUMMARY

In this paper we have presented results of a study of proton-antiproton annihilation into two and three pions in a baryon-exchange model. Specifically, we have taken into account

contributions from  $N$  exchange as well as from  $\Delta$  exchange consistently in the two- and three-pion annihilation channels. The free parameters of our model, the cutoff masses in the form factors at the  $NN\pi$  and  $N\Delta\pi$  vertices, were determined by the available experimental data on  $p\bar{p} \rightarrow \pi^+\pi^-$ . Thus, the results for the other annihilation channels considered,  $p\bar{p} \rightarrow \pi^0\pi^0$  as well as  $p\bar{p} \rightarrow \pi^+\pi^-\pi^0$  and  $p\bar{p} \rightarrow \pi^0\pi^0\pi^0$ , can be regarded as genuine predictions of the model.

The main aim of our work was to study and discuss the relative importance of  $NN$ ,  $N\Delta$  and  $\Delta\Delta$  exchanges for annihilation into three pions. For that purpose we prepared two sets of models which describe the cross sections of the reaction  $p\bar{p} \rightarrow \pi^+\pi^-$  with comparable quality but have dominant contributions from either  $N$  or  $\Delta$  exchange. In addition we employed three different analytical forms for the vertex form factors in order to explore the sensitivity of our results to these ingredients of our model.

It turned out that the contributions from annihilation diagrams involving the  $\Delta$  isobar are, in general, much less important for the three-pion channel than they are for annihilation into two pions. Specifically, for those models where the  $N$  exchange dominates the two pion decay we found the  $\Delta$ -exchange contributions to the three pion decay to be completely negligible. Even in those models where  $\Delta$  exchange plays a major role in the two-pion channel, there is only a moderate effect from the  $\Delta$  exchange in the three-pion channel. As a consequence, the total annihilation cross section into three uncorrelated pions is usually significantly larger if we assume that  $N$  exchange dominates the two-pion decay.

Not unexpectedly, the actual magnitude of the total three-pion annihilation cross section depends to a certain extent on the choice for the vertex form factors. This dependence is strongly reduced by requiring consistency between the treatment of the two- and three-pion decay channels, but ultimately cannot be avoided because it is already inherent in the specific functions used for the analytic forms of the form factor. With due concession for these uncertainties, our calculations show that the contributions of annihilation into three uncorrelated pions to the total three-pion annihilation cross section are by no means negligible. Indeed they might provide up to 10% of the total cross section for  $p\bar{p} \rightarrow \pi^+\pi^-\pi^0$  as well as for  $p\bar{p} \rightarrow 3\pi^0$ .

The results obtained in this work can also be invoked to assess the general viability of the baryon-exchange model of nucleon-antinucleon annihilation. Although the two-pion and uncorrelated three-pion final states make only rather tiny contributions to the total annihilation process, the relative sizes of the cross-sections for these two channels can be used as a hint to evaluate the possibility of describing most if not all of annihilation in the baryon-exchange framework. The cross sections for annihilation into two pions are of the order of a fraction of a millibarn in the energy region we have considered. The cross sections predicted by the baryon-exchange model for annihilation into three uncorrelated pions (taking a rough average of the extreme cases considered in this work, see Table III) are of the same order of magnitude. This is perhaps surprising since one might have thought that the need for more vertices and propagators – therefore more form factors – would suppress final states of more than two mesons in such models. Remembering that, according to the calculations of Ref. [9], annihilation into two mesons, summed over all meson types, amounts to about 30% of the total experimental annihilation cross section, it is tempting to generalize the results found here for pions to speculate that annihilation into three mesons, when summed over all meson types, could easily account for a similar percentage of the whole process.

Since it seems that multi-meson final states are not strongly suppressed in baryon-exchange models, states with four or more mesons could then easily account for the remaining of the cross section. Of course, such qualitative speculations could only be confirmed by detailed calculations, which would constitute a formidable task, but it can at least be claimed that the possibility of explaining the bulk of the annihilation process in a baryon-exchange picture is not ruled out.

#### ACKNOWLEDGMENTS

We would like to thank V. Mull for valuable discussions and the “Centro Nacional de Supercomputação da Universidade Federal do Rio Grande do Sul (UFRGS)”, where much of the computational work was done. Furthermore, we acknowledge communications with A.V. Anisovich concerning the  $p\bar{p} \rightarrow \pi^0\pi^0$  annihilation data. Financial support for this work was provided by the international exchange program DLR (Germany; BRA W0B 2F) - CNPq (Brazil; 910133/94-8), and by FAPERGS (Fundação de Amparo à Pesquisa do Estado do Rio Grande do Sul).

## REFERENCES

- [1] C. B. Dover, T. Gutsche, M. Maruyama, and A. Faessler, *Prog. Part. Nucl. Phys.* **29**, 87 (1992).
- [2] A. Amsler and F. Myhrer, *Ann. Rev. Nucl. Part. Sci.* **41**, 219 (1991).
- [3] C. Amsler, *Rev. Mod. Phys.* **70**, 1293 (1998); *Nucl. Phys.* **A663&664**, 93c (2000).
- [4] M. Maruyama and T. Ueda, *Nucl. Phys.* **A364**, 297 (1981); *Phys. Lett.* **124B**, 121 (1983).
- [5] A.M. Green and J.A. Niskanen, *Nucl. Phys.* **A412**, 448 (1984); *Nucl. Phys.* **A430**, 605 (1984).
- [6] A. Muhm, T. Gutsche, R. Thierauf, Y. Yan, and A. Faessler, *Nucl. Phys.* **A598**, 285 (1996) and references therein.
- [7] B. Moussallam, *Nucl. Phys.* **A407**, 413 (1983); *Nucl. Phys.* **A429**, 429 (1984).
- [8] T. Hippchen, J. Haidenbauer, K. Holinde, and V. Mull, *Phys. Rev. C* **44**, 1323 (1991); V. Mull, J. Haidenbauer, T. Hippchen, and K. Holinde, *Phys. Rev. C* **44**, 1337 (1991).
- [9] V. Mull and K. Holinde, *Phys. Rev. C* **51**, 2360 (1995).
- [10] Y. Yan and R. Tegen, *Phys. Rev. C* **54**, 1441 (1996).
- [11] Y. Yan and R. Tegen, *Nucl. Phys.* **A648**, 89 (1999).
- [12] M. Betz, E. A. Veit, V. Mull and K. Holinde, *Phys. Lett. B* **398**, 12 (1997).
- [13] M. Betz, E. A. Veit, J. Haidenbauer, and V. Mull, Proc. of *5<sup>th</sup> Rio de Janeiro International Workshop on Relativistic Aspects of Nuclear Physics*, ed. by T. Kodama, C.E. Aguiar, S.B. Duarte, Y. Hama, G. Odyniec, and H. Ströbele, (World Scientific, Singapore 1998), p. 403.
- [14] M. Betz, E.A. Veit, J. Haidenbauer, and V. Mull, Proc. of the *International Workshop on Hadron Physics 98*, ed. by E. Ferreira, F.F. de S. Cruz, and S.S. Avancini, (World Scientific, Singapore 1999), p. 377.
- [15] M. Betz, E.A. Veit, and J. Haidenbauer, Proc. of the *International Workshop on Hadron Physics 2000*, São Paulo, Brazil, April 2000, in print.
- [16] M. Foster et al., *Nucl. Phys.* **B6**, 107 (1968).
- [17] B. May et al., *Z. Phys. C* **46**, 191 (1990); **46**, 203 (1990).
- [18] C. Amsler et al., *Phys. Lett. B* **355**, 425 (1995) and references therein.
- [19] A. Abele et al., *Nucl. Phys.* **A609**, 562 (1996).
- [20] A. V. Anisovich et al., *Phys. Lett. B* **452**, 187 (1999).
- [21] Ch. Schütz, diploma thesis, Universität Bonn 1992; *Berichte des Forschungszentrums Jülich* No. 2733, 1992.
- [22] M. Benmerrouche, R. M. Davidson and N. C. Mukhopadhyay, *Phys. Rev. C* **39**, 2339 (1989).
- [23] R. Machleidt, K. Holinde, and Ch. Elster, *Phys. Rep.* **149**, 1 (1987); version given in Table 9 therein.
- [24] J. J. De Swart, *Rev. Mod. Phys.* **35**, 916 (1963).
- [25] B. C. Pearce, and B. K. Jennings, *Nucl. Phys.* **A528**, 655 (1991).
- [26] C. Schütz, J. W. Durso, K. Holinde, and J. Speth, *Phys. Rev. C* **49**, 2671 (1994).
- [27] F. Sai, S. Sakamoto, and S. S. Yamamoto, *Nucl. Phys.* **B213**, 371 (1983).
- [28] Y. Sugimoto et al., *Phys. Rev. D* **37**, 583 (1988).
- [29] G. Bardin et al., *Phys Lett. B* **192**, 471 (1987); in *Proceedings of the 1st Biennial*

*Conference on Low Energy Antiproton Physics*, Stockholm, 1990, edited by P. Carlson, A. Kerek, and S. Szilagyi (World Scientific, Singapore, 1991), p. 173.

- [30] A. Hasan et al., Nucl. Phys. **B378**, 3 (1992).
- [31] V. Mull, K. Holinde, and J. Speth, Phys. Lett. B **275**, 12 (1992).
- [32] V. Mull, G. Jansen, J. Speth, and K. Holinde, Phys. Lett. B **347**, 193 (1995).
- [33] R. S. Dulude et al., Phys. Lett. B **79**, 329 (1978); **79**, 335 (1978).
- [34] A. V. Anisovich et al., Phys. Lett. B **468**, 304 (1999).
- [35] A. V. Anisovich et al., Phys. Lett. B **471**, 271 (1999); Nucl. Phys. **A662**, 344 (2000).

## TABLES

TABLE I. Cutoffs (in MeV) for the various form factors used in the calculations. The first column gives the type of form factor; the second one identifies the corresponding set. The headings of the other columns specify the kind of cutoff.

Type	Set	$\Lambda_N$	$\Lambda_\Delta$
Monopole	A	1600	1300
Monopole	B	1250	1550
Gaussian	A	1300	1100
Gaussian	B	1100	1320
Pearce	A	1200	980
Pearce	B	1050	1250

TABLE II. Contributions to the  $p\bar{p} \rightarrow \pi^+\pi^-$  cross section (in  $\mu b$ ), calculated with different form factors (first column) and parameter sets (second column). The third column gives the laboratory kinetic energy (in MeV), the other columns different contributions, specified by the exchanged baryon(s) in the annihilation amplitude.

Form Factor	Set	Energy	$N$	$\Delta$	$N + \Delta$
Monopole	A	65	609	1.8	685
		220	322	1.1	332
Gaussian	A	65	559	6.2	663
		220	375	3.7	419
Pearce	A	65	571	25	782
		220	304	15	384
Monopole	B	65	66	436	741
		220	40	237	357
Gaussian	B	65	62	424	693
		220	54	260	414
Pearce	B	65	182	353	847
		220	104	189	404

TABLE III. Uncorrelated-channel contribution to the  $p\bar{p} \rightarrow \pi^+\pi^-\pi^0$  cross section (in  $\mu b$ ), calculated with different form factors (first column) and parameter sets (second column). The third column gives the laboratory kinetic energy (in MeV), the other columns list the various contributions.

Form Factor	Set	Energy	$NN$	$N\Delta$	$\Delta\Delta$	all
Monopole	A	65	309	$2.4 \cdot 10^{-2}$	$5.7 \cdot 10^{-5}$	310
		220	200	$1.7 \cdot 10^{-2}$	$4.4 \cdot 10^{-5}$	200
Gaussian	A	65	760	$3.5 \cdot 10^{-2}$	$1.3 \cdot 10^{-2}$	760
		220	535	$4.3 \cdot 10^{-1}$	$1.4 \cdot 10^{-2}$	535
Pearce	A	65	603	3.2	$2.4 \cdot 10^{-1}$	620
		220	404	2.8	$1.9 \cdot 10^{-1}$	403
Monopole	B	65	13	3.8	1.7	20
		220	8	2.5	1.2	12
Gaussian	B	65	67	12	9.4	84
		220	52	14	8.9	75
Pearce	B	65	138	22	46	242
		220	96	19	34	158

TABLE IV. Ratios of branching ratios for  $p\bar{p} \rightarrow \pi^+\pi^-\pi^0$ . The experimental values are taken from the phenomenological analysis of Ref. [17]. The theoretical results are obtained as relative cross sections at  $E_{lab} = 5$  MeV for different form factors and parameter sets.

	Form factor	Set	$^3S_1/{}^1S_0$	$^3P_1/{}^1P_1$	$^3P_2/{}^1P_1$
Model	Monopole	A	3.3	1.7	1.4
	Gaussian		3.2	1.5	1.1
	Pearce		3.9	1.7	1.8
Model	Monopole	B	3.2	24.3	7.9
	Gaussian		2.9	7.1	5.6
	Pearce		6.3	34.9	13.6
Experiment			1.9	2.9	3.8
State counting			3.0	1.0	1.67

TABLE V. Cross section for  $p\bar{p} \rightarrow \pi^0\pi^0$  at 600 MeV/c, integrated over angles from  $\cos(\theta) = 0$  to 0.85. The data is from Ref. [34].

Type	Set	cross section ( $\mu b$ )
Monopole	A	53.8
Monopole	B	106.9
Gaussian	A	80.7
Gaussian	B	119.8
Pearce	A	100.4
Pearce	B	126.5
Experiment		54.4

TABLE VI. The same as Table II for the  $p\bar{p} \rightarrow \pi^0\pi^0$  annihilation.

Form Factor	Set	Energy	$N$	$\Delta$	$N + \Delta$
Monopole	A	65	173	$8.1 \cdot 10^{-1}$	195
		220	62	$4.5 \cdot 10^{-1}$	70
Gaussian	A	65	232	3	283
		220	92	1.7	112
Pearce	A	65	257	11.9	359
		220	87	6.7	127
Monopole	B	65	21	197	328
		220	8	100	146
Gaussian	B	65	20	204	323
		220	13	120	175
Pearce	B	65	81	167	397
		220	29	83	167

TABLE VII. Uncorrelated contribution to the cross section for  $p\bar{p} \rightarrow \pi^0\pi^0\pi^0$  at  $p_{lab} = 600$  MeV/c, calculated with different form factors and parameter sets. Note that the experimental total annihilation cross section (which includes the uncorrelated as well as correlated contributions) is  $356 \pm 18 \mu b$  [20].

Type	Set	$\sigma(\mu b)$
Monopole		13.5
Gaussian	A	37.8
Pearce		31.8
Monopole		2.2
Gaussian	B	7.2
Pearce		16.0

TABLE VIII. The same as Table III for the  $p\bar{p} \rightarrow \pi^0\pi^0\pi^0$  annihilation. All cross sections are given in  $\mu b$ .

Form Factor	Set	Energy	$NN$	$N\Delta$	$\Delta\Delta$	all
Monopole	A	65	24	$9.6 \cdot 10^{-3}$	$8.4 \cdot 10^{-7}$	25
		220	11	$4.3 \cdot 10^{-3}$	$4.9 \cdot 10^{-7}$	12
Gaussian	A	65	73	0.097	$3.3 \cdot 10^{-4}$	74
		220	32	0.060	$2.6 \cdot 10^{-4}$	31
Pearce	A	65	51	1.2	$3.6 \cdot 10^{-3}$	60
		220	23	0.53	$2.4 \cdot 10^{-3}$	27
Monopole	B	65	1.0	1.6	0.025	4.2
		220	0.46	0.75	0.014	1.9
Gaussian	B	65	7.8	4.3	0.22	14
		220	3.6	2.2	0.15	6.4
Pearce	B	65	12	9.7	0.53	31
		220	5.6	4.6	0.32	14

## FIGURES

FIG. 1. Born transition amplitude for  $N\bar{N} \rightarrow 2\pi$ .

FIG. 2. Born transition amplitude for  $N\bar{N} \rightarrow 3\pi$ .

FIG. 3. Elastic part of the  $N\bar{N}$  interaction.

FIG. 4. Microscopic (a) and phenomenological (b) annihilation part of the  $N\bar{N}$  interaction.

FIG. 5. Transition potential for  $N\bar{N} \rightarrow 2$  mesons.

FIG. 6.  $p\bar{p} \rightarrow \pi^+\pi^-$  cross sections. The solid lines, long dashed lines and short dashed lines correspond to our results with the monopole, Gaussian and Pearce form factors. At left (right), results with parameter set A (B). The data are from Ref. [27–29].

FIG. 7.  $p\bar{p} \rightarrow \pi^+\pi^-$  differential cross sections for  $p_{lab} = 360$  MeV/c and for  $p_{lab} = 679$  MeV/c. Same description of the curves as in Fig. 6. Experimental data are taken from Ref. [30].

FIG. 8.  $p\bar{p} \rightarrow \pi^+\pi^-\pi^0$  cross section as a function of the incident momentum. The sums of two-meson channels [9] plus our results for the three uncorrelated-pion channel with the various types of form factors and parameter sets stated in Table I lie inside the shadowed area. Experimental data are taken from Ref. [27].

FIG. 9.  $p\bar{p} \rightarrow \pi^0\pi^0$  differential cross sections for  $p_{lab} = 360$  MeV/c and for  $p_{lab} = 600$  MeV/c. The same description of the curves as in Fig. 6. Experimental data are taken from Ref. [34].

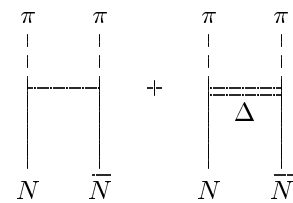


FIG. 1

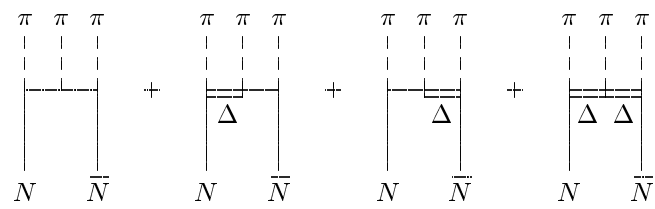


FIG. 2

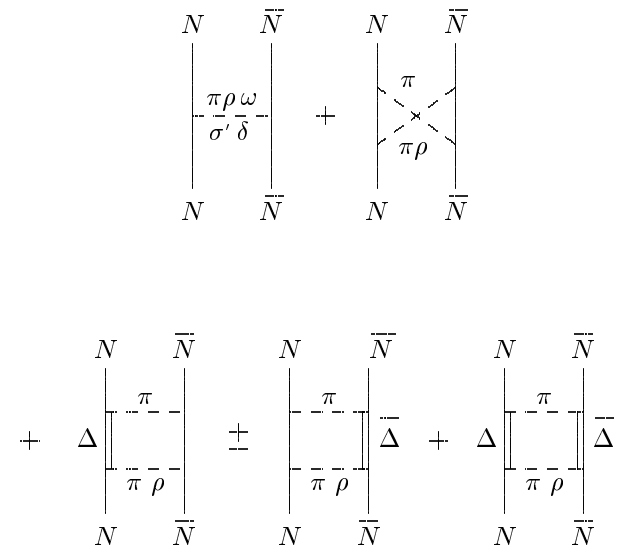


FIG. 3

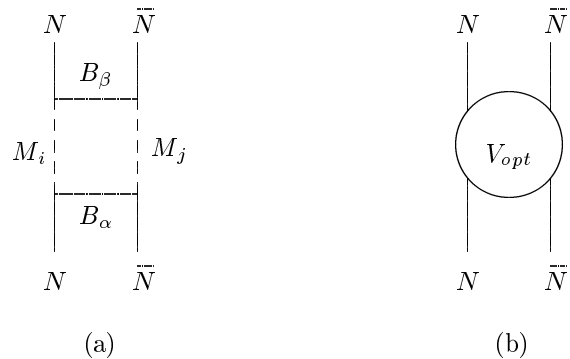
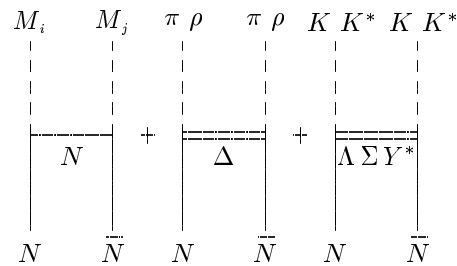


FIG. 4



$M_i, M_j = \pi, \eta, \rho, \omega, f_0, a_0, f_1, a_1, f_2, a_2$

FIG. 5

FIG. 6

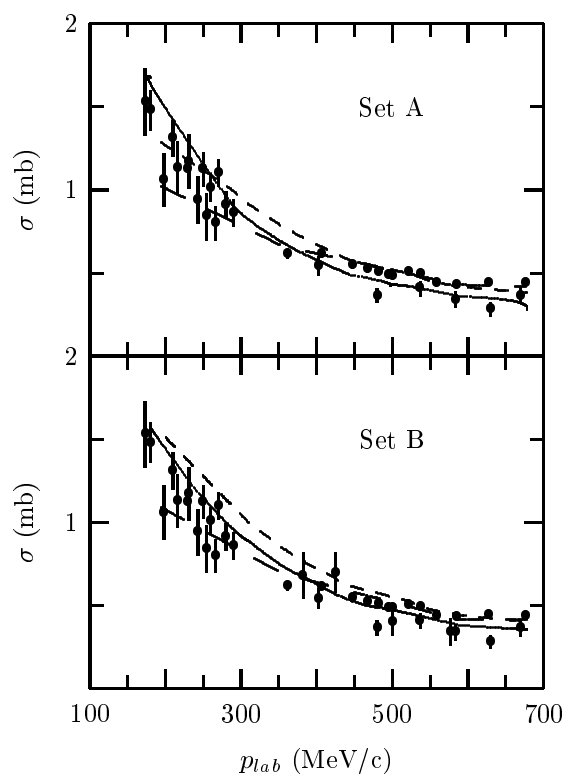


FIG. 7

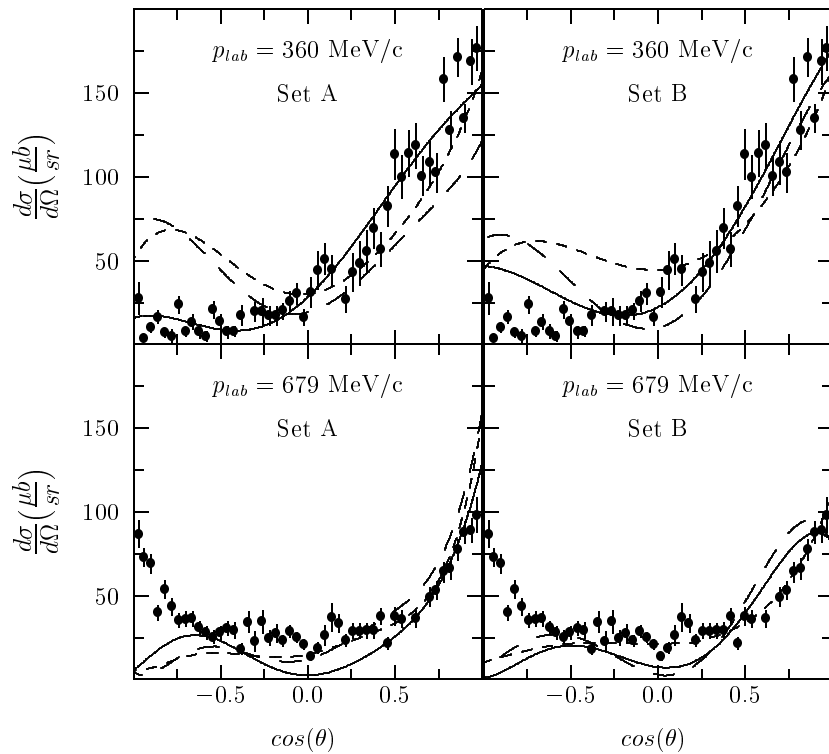


FIG. 7

FIG. 8

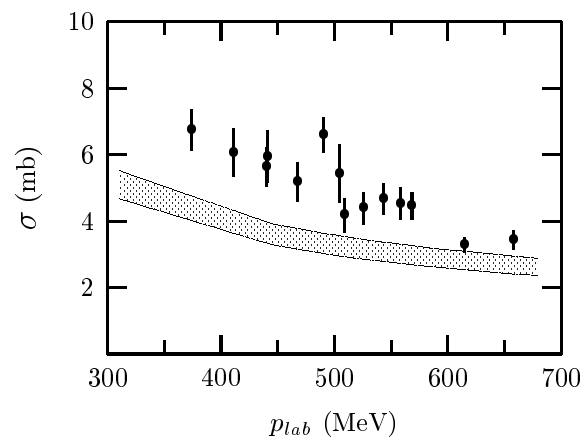


FIG. 8

FIG. 9

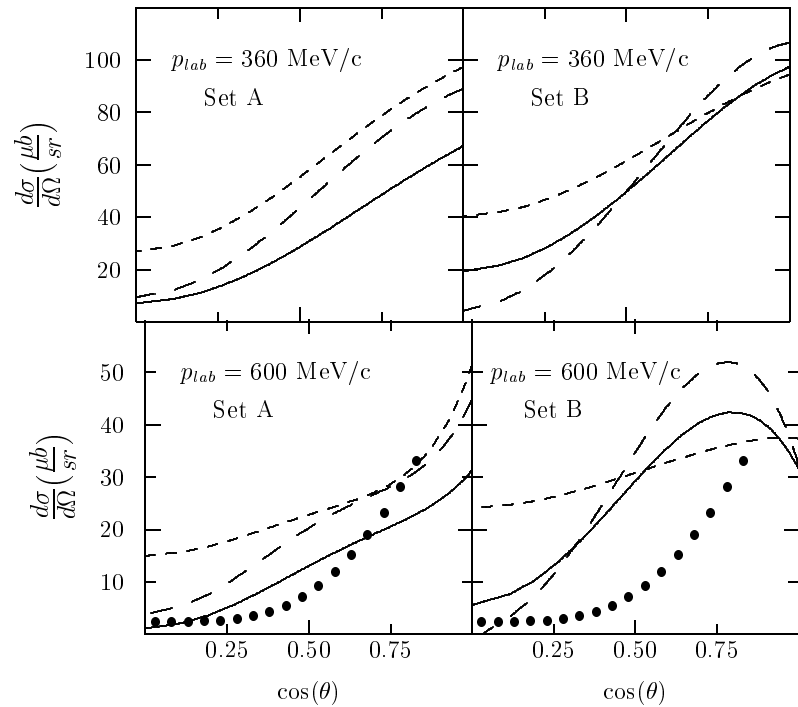


FIG. 9